

High critical current density and improved flux pinning in bulk MgB₂ synthesized by Ag addition

Chandra Shekhar ^{a)}, Rajiv Giri, R. S. Tiwari and O. N. Srivastava

Department of Physics Banaras Hindu University, Varanasi-221005, India

S. K. Malik

Tata Institute of Fundamental Rresearch, Mumbai-400005, India

ABSTRACT

In the present investigation, we report a systematic study of Ag admixing in MgB₂ prepared by solid-state reaction at ambient pressure. All the samples in the present investigation have been subjected to structural/ microstructural characterization employing x-rays diffraction (XRD) and transmission electron microscopic (TEM) techniques. The magnetization measurements were performed by physical property measurement system (PPMS). The TEM investigations reveal the formation of MgAg nanoparticles in Ag admixed samples. These nanoparticles may enhance critical current density due to their size (~ 5-20 nm) compatible with coherence length of MgB₂ (~ 5-6 nm) . In order to study the flux pinning effect of Ag admixing in MgB₂, the evaluation of intragrain critical current density (J_c) has been carried out through magnetic measurements on the fine powdered version of the as synthesized samples. The optimum result on intragrain J_c is obtained for 10 at.% Ag admixed sample at 5K. This corresponds to $\sim 9.23 \times 10^7$ A/cm² in self-field, $\sim 5.82 \times 10^7$ A/cm² at 1T, $\sim 4.24 \times 10^6$ A/cm² at 3.6T and $\sim 1.52 \times 10^5$ A/cm² at 5T. However, intragrain J_c values for MgB₂ sample without Ag admixing are $\sim 2.59 \times 10^6$ A/cm², $\sim 1.09 \times 10^6$ A/cm², $\sim 4.53 \times 10^4$ A/cm² and 2.91×10^3 A/cm² at 5 K in self field, 1T, 3.6T and 5T respectively.. The high value of intragrain J_c for Ag admixed MgB₂ superconductor has been attributed to the inclusion of MgAg nanoparticles into the crystal matrix of MgB₂, which are capable of providing effective flux pinning centres. A feasible correlation between microstructural features and superconducting properties has been put forward.

^{a)}Electronic mail: chand_bhu@yahoo.com

INTRODUCTION

The recent discovery of superconductivity in intermetallic compound MgB₂ has generated tremendous interest because of its potential for applications at high magnetic field ^{1,2}. The critical current density (J_c) and upper critical field (H_{c2}) are two most important parameters of any superconductor for practical applications. MgB₂ possesses higher upper critical field than that of conventional superconductors (NbTi, Nb₃Sn etc.). It appears to be the first promising intermetallic superconductor for applications in temperature range 20-30 K at high magnetic field ^{3,4}. Another important feature of MgB₂ is that now it is believed that unlike high temperature cuprate superconductors MgB₂ does not contain intrinsic obstacles to current flow between the grains ⁵. Evidence for strongly coupled grains have been found even for randomly aligned, porous and impure samples ^{6,7}, thus providing high feasibility of scaling up the material to form shapes like wires and tapes ⁸⁻¹⁰. Large engineering applications have been hampered so far by low density and poor flux pinning behaviour of MgB₂ which induces degradation of J_c in high magnetic fields. Many researchers have attempted to improve the flux pinning behaviour through several types of processes such as high energy ion-irradiation ¹¹, chemical doping using different metallic and non-metallic phases and nano particles admixing ¹²⁻¹⁴. Recent studies have shown that chemical doping may be effective and feasible approach for increasing critical current density of MgB₂ superconductors ¹⁵⁻¹⁸. Therefore, it is necessary to study doping effect of suitable elements in MgB₂. This may open wide spread applications of MgB₂. In our recent study doping of La in MgB₂ has been found to increase critical current density due to LaB₆ nanoparticle inclusions in MgB₂ matrix ¹⁵.

Several researchers have reported the enhancement of J_c by chemical doping. Dou et al., in a series of papers¹⁹⁻²¹ have shown that SiC and carbon nanoparticle doping significantly improves J_c & irreversibility field (H_{irr}). Mastsumoto *et al*²² have reported enhancement of J_c and H_{irr} through SiO₂ and SiC doping.

In earlier studies Ag admixing has been reported to result in enhancement of critical current density in cuprate superconductors²³⁻²⁵. Recently studies on synthesis and superconducting characteristics of Ag admixed MgB₂ have been reported²⁶⁻²⁸. In these studies, authors have focused their investigation on low concentration of Ag admixed MgB₂ compound only and reported low critical current density e.g. Kumar *et al.* have observed intragrain J_c value $\sim 1.5 \times 10^5$ A/cm² at 5K and in zero field²⁶. However, a detailed investigation of role of Ag admixing in MgB₂ in rather wider compositional range leading to maximum enhancement of J_c and H_{irr} has not been carried out so far. In the present investigation, we have made an effort to find out optimum level and condition of admixing of Ag in MgB₂. Structural and microstructural characterization of Ag admixed MgB₂ superconductor has been done and the flux pinning capability of Ag has been explored. Based on the magnetization measurements, we have evaluated intragrain critical current density (J_c), behaviour of pinning force density (F_p) and upper critical field (H_{c2}) for Ag admixed samples.

EXPERIMENTAL DETAILS

Ag admixed MgB₂ bulk samples with nominal composition MgB_{2-x} at.% Ag ($0 \leq x \leq 30$ at.%) have been synthesized by solid-state reaction method at ambient pressure using high purity powders of Mg (99.9%), B (99%) and Ag (99.9%). The particles size of starting Mg, B and Ag powders are in the range of 30-40 μ m, $\sim 5\mu$ m and 4-7 μ m respectively. These powders were fully mixed and cold pressed (3.5 tons/ inch²) into small rectangular pellets (10 x 5 x 1 mm³). Thereafter, the pellets were encapsulated in a Mg metal cover to take care of Mg loss and avoid the formation of MgO during the sintering process. The pellet configuration was wrapped in a Ta foil and sintered in flowing Ar atmosphere in a programmable tube type furnace at 900^oC for 2 hour. The pellets were cooled to room temperature at the rate of 5^oC/ min. The encapsulating Mg cover was then removed and Ag added MgB₂ samples were retrieved for further studies. This encapsulation technique has been developed in our laboratory to synthesize MgB₂ superconductors¹⁵.

All the samples in the present investigation were subjected to gross structural characterization by powder x-ray diffraction technique (XRD, PANalytical X[`] Pert Pro, CuK _{α}) and microstructural characterization by transmission electron microscope (Philips EM-CM-12). The magnetization (M) measurements have been carried out at Tata Institute of Fundamental Research (Mumbai, India) over a temperature range of 5-40K employing a physical property measurement system (PPMS, Quantum Design) on fine ground powders of the as synthesized samples. Intragrain J_c was calculated from the height ' ΔM ' of the magnetization loop (M-H) using Bean's formula based on critical state model²⁹. It should be pointed out the Bean's formula leads to the optimum estimate of intragrain J_c for superconductors having weakly coupled grains. However, this model will be appropriate for optimum estimation of J_c in case of MgB₂ (where grains are strongly coupled) only when magnetization measurements are carried out on fine powder of the as synthesized sample. In the fine powder form, strong coupling is non-existent. Therefore, the J_c can be estimated employing Bean's formula and using average size of the powder particles. It may be pointed out that fine ground particles usually correspond to agglomerates of nearly spherical shape ($\sim 5\mu$ m) covering only few grains (as estimated by scanning electron microscope SEM). Thus in the present investigation, we have used the average size of the powder particle ($\sim 5\mu$ m).

$$J_c = \frac{30\Delta M}{\langle d \rangle}$$

Where ' ΔM ' is the height of hysteresis loop in emu/cm³ and $\langle d \rangle$ is the average particle size in cm ($\sim 5\mu$ m).

RESULTS AND DISCUSSION

The representative x-ray diffraction patterns of Ag admixed MgB₂ samples are shown in Fig.1 The XRD patterns reveal that all the samples are polycrystalline in nature and correspond to

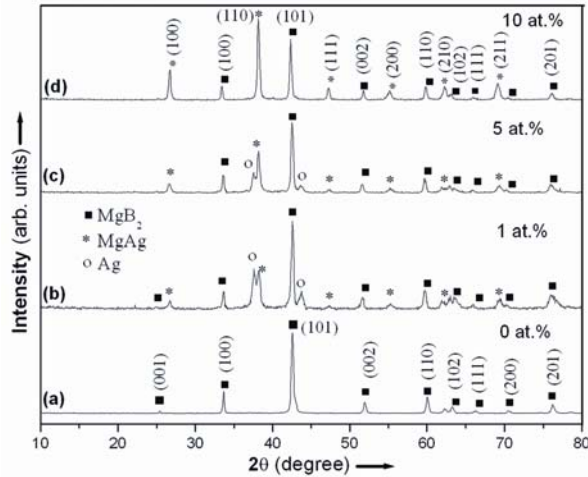


Fig 1 Representative powder XRD patterns of MgB_2-x at.% Ag ($x=0, 1, 5$ & 10 at.%).

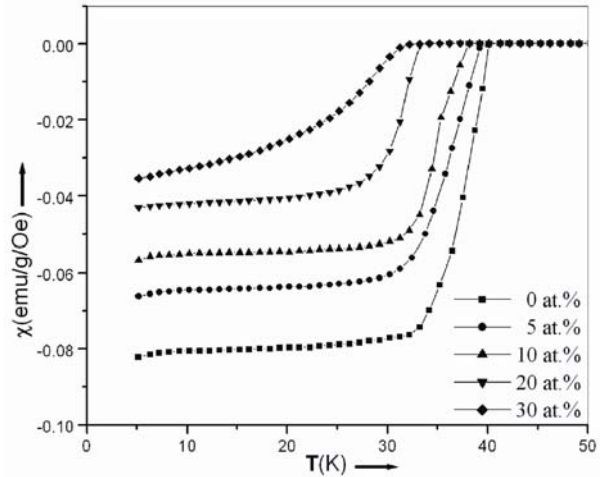


Fig 2 Temperature dependent dc magnetic-susceptibility (χ) behavior of MgB_2-x at.% Ag ($0 \leq x \leq 30$ at.%)

hexagonal structure of MgB_2 ($a=b=3.08\text{\AA}$, $c = 3.52\text{\AA}$). Any appreciable change in the lattice parameters of Ag admixed MgB_2 samples (using a computerized programme based on least square fitting method) has not been found within the experimental limit of 0.001\AA . It may be noticed that Ag admixed MgB_2 samples have some additional peaks. These additional peaks have been indexed to both Ag and MgAg for lower Ag concentration ($Ag < 10$ at.%). However, for the higher Ag concentration ($Ag \geq 10$ at.%), these additional peaks get explicable in terms of MgAg only. Unlike the case when Ag concentration is very small, for higher Ag concentration ($Ag \geq 10$ at.%) the interfacial area of Mg/Ag will be large facilitating the interdiffusion of Ag into Mg. This will lead to consumption of all Ag leading to the formation of MgAg phase only.

The dc magnetic susceptibility (χ) of MgB_2-x at.% Ag (with $0 \leq x \leq 30$ at.%) samples are shown in Fig.2 for 50 Oe field as a function of temperature. Based on this the transition temperature of MgB_2 admixed with different concentration of Ag can be taken to lie between 32 -40K. The decrease in T_c with increasing concentration of Ag in the samples may be due to the presence of secondary phases (Ag, MgAg) in the sample.

The central aim of the present investigation is to explore the flux pinning properties and magnetic behaviour of Ag admixed MgB_2 samples and their possible correlation with microstructural features. We therefore, first describe various microstructural features induced by different admixing concentrations of Ag in MgB_2 . Thereafter, evaluation of critical current density and behaviour of flux pinning force through magnetic measurements will be elucidated. Finally correlation between intragrain J_c and microstructural features will be described and discussed. The microstructural characterization has been carried out by transmission electron microscope in both imaging and diffraction mode of the as synthesized Ag admixed. MgB_2 samples with different Ag concentration. Fig.3(a) shows the representative transmission electron micrograph for MgB_2 compound. The selected area diffraction (SAD) pattern corresponding to the TEM micrograph is shown Fig.3(b), which reveals the hexagonal lattice pattern corresponding to MgB_2 compound.

With admixing of Ag in MgB_2 the dominant and specific microstructural feature is the occurrence of MgAg secondary nanoparticles, which are found to be invariably present. For example the presence of MgAg nanoparticles can be easily discernible from the representative TEM micrograph of MgB_2-10 at.% Ag compound [Fig.3(c)]. The density of the nanoparticles is higher at grain boundaries in comparison to within the MgB_2 grains. The average size of the nanoparticles inclusions has been found to be in the range of 5-20nm. Such a preferential presence of nanoparticles at grain boundaries (GBs) may be understood in term of interaction of grain boundary (GB) with the MgAg nanoparticles. It may be pointed out that the GBs are disordered region in crystals. GBs therefore, represent high-energy configurations. Because of the Coulomb interaction between GB and the impurity atoms, GB tends to attract the impurity atoms in order to decrease its energy. It should

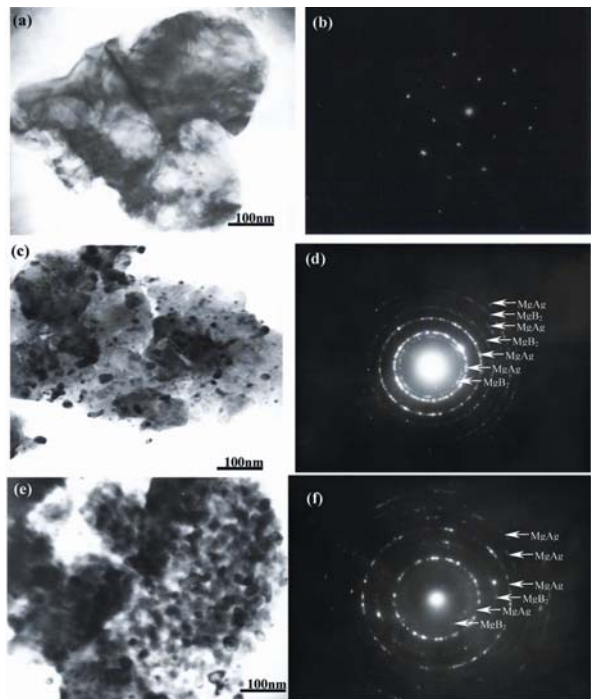


Fig 3 (a) The representative TEM micrograph of pure MgB_2 . (b) Selected area diffraction (SAD) pattern of hexagonal lattice corresponding to MgB_2 grain.

(c) Presence of $MgAg$ nanoparticles discernible from the TEM micrograph of MgB_2 –10 at.% Ag admixed sample. (d) SAD pattern corresponding to TEM micrograph of fig.3 (a) shows spotty ring pattern which corresponds to MgB_2 and $MgAg$ nanoparticles (e) Representative TEM micrograph corresponding to MgB_2 –30 at.% Ag admixed sample depicting significant precipitation of $MgAg$. (f) SAD pattern corresponding to TEM micrograph of fig. 3(e) has been indexed for MgB_2 and $MgAg$.

While diffusion of Ag to the GB forming $MgAg$ is easy because it will be quite difficult for Ag to diffuse into the grain because of large difference in the size of Mg and Ag . However, some of the Ag atoms would still diffuse into the grain because of Mg vacancies present in the grain and would form $MgAg$. Therefore, the chemical dopants have a higher probability to stay at the GB region. The SAD pattern corresponding to TEM micrograph [shown in Fig. 3(d)] reveals the spotty ring pattern. These diffraction rings, which correspond to MgB_2 and $MgAg$ nanoparticles, depict the inclusion of nanoparticles in MgB_2 .

The TEM micrograph for MgB_2 –30 at.% Ag sample revealing the very high density of $MgAg$ nanoparticles is discernible from the Fig. 3(e). It is interesting to note that distribution of $MgAg$ nanoparticle for this sample is different from that of the MgB_2 –10 at.% Ag sample. In this case density of nanoparticles is high within the MgB_2 grain. Such a feature may be due to high admixing concentration of Ag in MgB_2 . The representative SAD pattern of MgB_2 –30 at.% Ag [shown in Fig. 3(f)] have been indexed for MgB_2 and $MgAg$. Thus, it may be suggested that for lower concentration i.e. $x \leq 10$ at.%, there will be smaller concentration of $MgAg$ in MgB_2 matrix in comparison to the grain boundaries. Upto this concentration of Ag (i.e. $x \sim 10$ at.%), size and density of nanoparticles are suitable to act as flux pinning centres. When the Ag concentration is high i.e. $x > 10$ at.% significant precipitation/ segregation of $AgMg$ results in the sample. Such a presence of high density of secondary phases leads to the suppression of superconductivity. It is interesting to notice that the definite formation of $MgAg$ has been established through both XRD & SAD pattern (see Fig 1 & 3). The exact reason of the formation of $MgAg$ is not clear so far. However, it appears that the most feasible reason for the formation of $MgAg$ is the reaction of excess Mg with Ag . It may be pointed out that in the present investigation, as outlined in experimental section, excess Mg was invariably taken to take care of Mg loss and also avoid the formation of MgO .

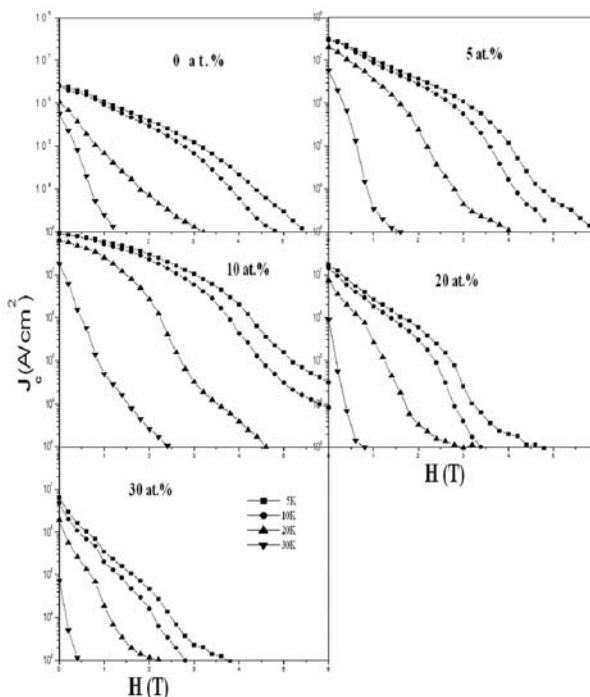


Fig 4 Intragrain J_c as a function of applied magnetic field for MgB_2 – x at.% Ag ($0 \leq x \leq 30$ at.%) at 5, 10, 20 and 30K.

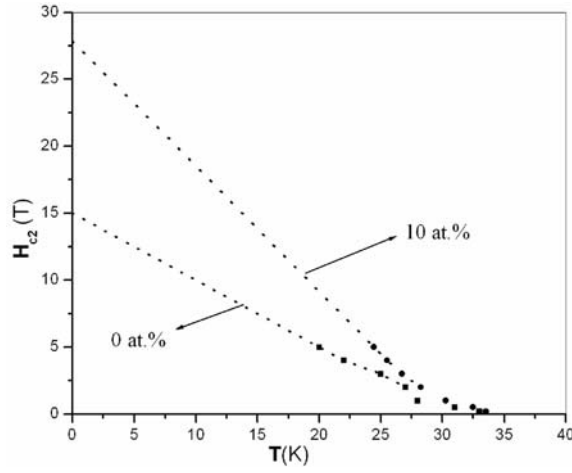


Fig 5 The extrapolated upper critical field as a function of temperature for MgB_2 and MgB_2-10 at.% Ag admixed samples.

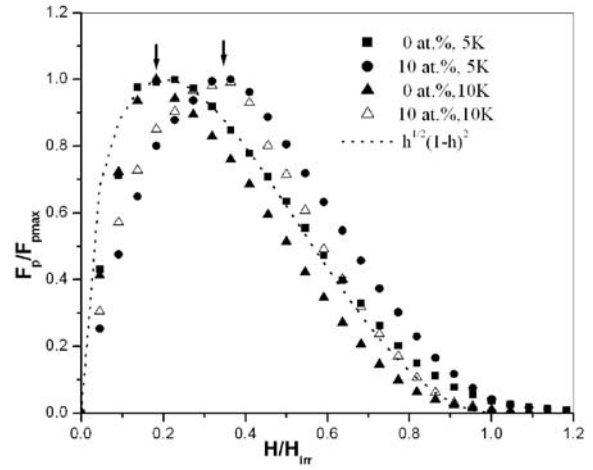


Fig 6 Normalized pinning force F_p/F_{pmax} as a function of reduced magnetic field for MgB_2 and MgB_2-10 at.% Ag admixed samples at 5 & 10K. Shifting of peak position from Kramer plot towards higher magnetic field reveals the presence of extra pinning centres in Ag added MgB_2 sample.

The magnetization measurements as a function of applied magnetic field (H) have been carried out at 5, 10, 20 and 30K, for each sample. The intragrain J_c as a function of applied magnetic field MgB_2-x at.% Ag samples are shown in Fig. 4. It is clear from J_c versus H curves that the intragrain J_c of 10 at.% Ag sample attains the highest value among all the samples for all temperatures upto 30K and for the whole field region up to 5T. It appears from the present investigation that this sample contains optimum density of MgAg nanoparticles at GB as well as within the grain of MgB_2 . For example at 5K, intragrain J_c for 10 at.% Ag added sample is $\sim 9.23 \times 10^7$ A/cm² in self-field, $\sim 5.82 \times 10^7$ A/cm² at 1T, $\sim 4.24 \times 10^6$ A/cm² at 3.6T and $\sim 1.52 \times 10^5$ A/cm² at 5T. The intragrain J_c values for MgB_2 sample without Ag admixing are $\sim 2.59 \times 10^6$ A/cm², $\sim 1.09 \times 10^6$ A/cm², $\sim 4.53 \times 10^4$ A/cm² and 2.91×10^3 A/cm² at 5 K in self field, 1T, 3.6T and 5T respectively. The above clearly shows that Ag admixing has resulted in enhancement of intragrain J_c for all fields. This is consistent with microstructural characterization. As already outlined Ag admixing ≥ 10 at.% leads to the presence of discrete particles within the grain. The size of these particles is broadly compatible with the coherence length $\sim 60\text{\AA}$. Similar variations of J_c with magnetic fields were also observed for temperature 10, 20 and 30 K also. It should be pointed out that the value of J_c found for 10 at.% in the present study is significantly higher than the values reported by earlier workers²⁶. The values of H_{c2} , determined as the field at which M (H) first deviated from the background, as a function of temperature are shown in Fig. 5. The extrapolation of the curve gives the H_{c2} value at 0K. The H_{c2} value at 0K for MgB_2 sample without Ag is ~ 15 T and for 10at.% Ag admixed MgB_2 sample is ~ 28 T. These values of H_{c2} are also close to the values obtained by Werthamer Helfand- Hohenberg model³⁰

$$H_{c2}(0) = 0.7 T_c \left(\frac{dH_{c2}}{dT} \right)$$

which yields 16T and 30T as $H_{c2}(0)$ values for pure MgB_2 and 10at.% Ag respectively.

The flux pinning mechanism associated with microstructural defects is often assessed by analyzing the slope of flux pinning force, $F_p(H)$, as a function of temperature. The normalized pinning force F_p / F_{pmax} plotted against a reduced field h, ($h = H/H_{irr}$) typically overlap when a single pinning mechanism and pinning centre is dominant³¹. The irreversibility field (H_{irr}) has been estimated by extrapolating the $J_c^{1/2}H^{1/4}$ versus H curve to the horizontal axis. This technique (also

called Kramer extrapolation) provides usually a very good estimate of H_{irr}^{32} . In the present study the values of H_{irr} at 10K are 4.7T and 5.8T for pure MgB_2 and optimally Ag admixed (10 at%) MgB_2 respectively. Such scaling behaviour is commonly observed in intermetallic low temperature superconductor (e.g. Nb_3Sn , $NbTi$)³³. This pinning mechanism is governed by the shear modulus³² and produces a bulk pinning force $F_p(H) = \mu_0 H J_c(H)$ with the characteristics field dependence proportional to $h^{1/2} (1-h)^2$ ³⁴, where h is reduced magnetic field. In the present investigation there is a slight but clear shift of the peak of the pinning force towards higher field [see Fig. 6]. Such a shift of the peak of the pinning force is indication of the presence of additional pinning centres. Recently Cooley et al have shown that deviation from the usual flux shear behaviour is due to core pinning by small precipitation such as MgO nano precipitates in MgB_2 thin film³⁵. Therefore, in the present study deviation of peak position from Kramer plot i.e. shifting of flux pinning force peak towards higher field, may be attributed to the nano inclusion of MgAg, which are expected to provide extra flux pinning force.

CONCLUSION

In conclusion, we have successfully synthesized Ag admixed MgB_2 sample at ambient pressure. In the present investigation exploration of microstructural features induced by admixing of Ag in MgB_2 compound and its correlation with intragrain J_c have been carried out. The highest value of J_c at 5K [$\sim 9.23 \times 10^7$ A/cm² in self field, $\sim 5.82 \times 10^7$ A/cm², $\sim 4.24 \times 10^6$ A/cm² and $\sim 1.52 \times 10^6$ A/cm² at fields of 1T, 3.6T and 5T respectively] has been obtained for 10at.% sample. This enhancement of J_c has been found to result due to optimum size and density of MgAg nanoparticles inclusions in MgB_2 . The study of nature of flux pinning force shows a shift in peak positions from Kramer plot, which is due to core pinning by MgAg nanoparticles. This shifting of peak position leads us to conclude that the additional pinning centres are present in the samples in the form of MgAg nanoparticles

ACKNOWLEDGEMENTS

The authors are grateful to Prof. A.R. Verma, Prof. C.N.R. Rao, Prof. S.K. Joshi and Prof. A.K. Roychaudhary for fruitful discussion and suggestions. Financial supports from UGC, DST-UNANST and CSIR are gratefully acknowledged. One of the authors Rajiv Giri is thankful to CSIR New Delhi, Govt. of India for awarding SRF (Ext.) fellowship.

REFERENCES

1. J. Nagamatsu, N. Norimasa, T. Muranaka, Y. Zenitani and J. Akimitsu, *Nature* **410**, 63 (2001).
2. D. C. Larbalestier et al *Nature* **410**, 186 (2001).
3. L. Chen, et al, *Appl. Phys. Lett* **88**, 262502 (2006),
4. H. Fang, P. Gijavanekar, Y. X. Zhou, P. T. Putman, K Salama, *IEEE Trans. Applied Superconductivity* **15**, 3200 (2005).
5. Y. Bugoslavsky, G. K. Perkins, X. Qi, L. F. Cohen and A. D. Caplin, *Nature* **410**, 5639 (2001).
6. P. C. Canfield, D. K. Finnemore, S. L. Bud'ko, J. E. Ostenson, G. Lapertot, C. E. Cunningham, and C. Petrovic, *Phys. Rev. Lett.* **86**, 2423 (2001).
7. S. Jin, H. Mavoori, C. Bower and R. B. van Dover, *Nature* **411**, 563 (2001).
8. M. D. Sumption, M. Bhatia M. Rindfleisch, M. Tomsic S. Soltanian, S. X. Dou and E. W. Collings *Appl. Phys. Lett.* **86**, 092507 (2005).
9. Y. Feng, Y. Zhao, A. K. Pradhan, L. Zhou, P. X. Zhang, X. H. Liu, P. Ji, S. J. Du, C. F. Liu, Y. Wu and N. Koshizuka, *Supercond. Sci. Technol.* **15** 12 (2002)
10. T. Nakane, C. H. Jiang, T. Mochiku, H. Fujii, T. Kuroda and H. Kumakura *Supercond. Sci. Technol.* **18** 1337 (2005).
11. I. Pallecchi, C. Tarantini, H. U. Aebersold, V. Braccini, C. Fanciulli, C. Ferdeghini, F. Gatti, E. Lehmann, P. Manfrinetti, D. Marré, A. Palenzona, A. S. Siri, M. Vignolo, and M. Putti, *Phys. Rev. B* **71**, 212507 (2005).
12. E. M. Choi, H. S. Lee, H. Kim, S. I. Lee, H. J. Kim and W. N. Kang *Appl. Phys. Lett.* **84**, 82 (2004).
13. Y. Zhao C. H. Cheng L. Zhou Y. Wu, T. Machi, Y. Fudamoto, N. Koshizuka, and M. Murakami, *Appl. Phys. Lett.* **79**, 1154 (2001).

14. S. F. Wang, S.Y. Dai, Y.L. Zhou, Y.B. Zhu, Z.H. Chen, H.B. Lü and G.Z. Yang, *Journal of Superconductivity* **17**, 397 (2004).
15. Chandra Shekhar, RajivGiri, R. S.Tiwari, D. S. Rana, S. K. Malik and O. N. Srivastava, *Supercond. Sci. Technol.* **18**, 1210 (2005).
16. J. Wang, Y. Bugoslavsky, A. Berenov, L. Cowey, A. D. Caplin, L. F. Cohen, J. L. MacManus Driscoll, L. D. Cooley, X. Song, and D. C. Larbalestier, *Appl. Phys. Lett.* **81**, 2026 (2002).
17. T. M. Shen, G. Li, X. T. Zhu, C. H. Cheng and Y. Zhao *Supercond. Sci. Technol.* **18**, L49 (2005).
18. M. Bhatia, M. D. Sumption, E. W. Collings, and S. Dregia, *Appl. Phys. Lett.* **87**, 042505 (2005).
19. S. X. Dou, S. Soltanian, J. Horvat, X. L. Wang, S. H. Zhou, M. Ionescu, and H. K. Liu P. Munroe M. Tomsic, *Appl. Phys. Lett.* **81**, 3419 (2002).
20. A. V Pan, S. Zhou, H. Liu and S. Dou, *Supercond. Sci. Technol.* **16**, 639 (2003).
21. S. X. Dou, W. K. Yeoh, J. Horvat, and M. Ionescu, *Appl. Phys. Lett.* **83**, 4996 (2003).
22. A. Matsumoto, H. Kumakura, H. Kitaguchi and H. Hatakeyama, *Supercond. Sci. Technol.* **16**, 926 (2003).
23. Y. Zhao, C. H. Cheng and J. S. Wang, *Supercond. Sci. Technol.* **18**, S34 (2005).
24. O. Görür, C. Terzioglu, A. Varilci and M. Altunbas, *Supercond. Sci. Technol.* **18**, 1233 (2005).
25. G. Plesch, F. Hanic, A. Cigan, J. Manka, A. Buckuliakova, S. Buchta, *Int. J. Inorganic Mater* **3**, 537 (2001).
26. D. Kumar, S. J. Pennycook, J. Narayan, H. Wang and A. Tiwari, *Supercond. Sci. Technol.* **16**, 455(2003).
27. J.D. Guo, X.L. Xu, Y.Z. Wang, L. Shi and D.Y. Liu, *Material Letters* **58**, 3707(2004).
28. M. Zouaoui, A. M'chirgui, F. B. Azzouz, B. Yangui and M. Ben Salem, *Physica C* **383**, 217 (2002).
29. C.P.Bean, *Rev. Mod. Phys.* **36**, 31 964).
30. E. Helfand and N. R. Werthamer, *Phys. Rev.* **147**, 288 (1996).
31. W. A. Fietz, W. W. Webb, *Phy. Rev.* **178**, 657(1969).
32. E. J. Krammer, *J Appl Phys* **44**, 1360 (1973).
33. L. D. Cooley and P. J. Lee, *IEEE Trans. Applied Superconductivity*, **11**, 3820 (2001).
34. A. Kahan, *Phys. Rev. B* **43**, 2678 (1991).
35. L. Cooley, S. Xueyan, D. Larbalestier, *IEEE Trans. Applied Superconductivity*, **13**, 3280 (2003).